288. Directional conjugate smoothing for analysis of axi-symmetric fluid vibrations

J. Ragulskienė[1], J. Maciulevičius[1], R. Maskeliūnas[2], L. Zubavičius[2]
[1]Kaunas College, Department of Technical Sciences,
Pramonės 20, LT-50468 Kaunas, Lithuania
e-mail: jurate352@gmail.com
[2]Vilnius Gediminas Technical University, Department of Printing Machines,
J. Basanavičiaus 28, LT-03224 Vilnius, Lithuania
E-mail: *Rimas.Maskeliunas@me.vgtu.lt, Leonas.Zubavicius@me.vgtu.lt*

(Received 11 June 2007; accepted 20 August 2007)

Abstract. Numerical implementation of the Abel transform for the construction of digital fluid holographic images is analyzed in this paper. Volumetric strains are obtained from the numerical calculations using the displacement formulation by the method of finite elements. Then the field of volumetric strain is obtained by using the procedure of conjugate approximation with smoothing. Numerical procedure is developed for the calculation of the Abel transform on the basis of the right rectangle numerical integration rule and thus the digital holographic image is constructed. The obtained digital holographic images are used in the hybrid experimental – numerical procedure for the determination of the correlation with the experimental holographic images.

Keywords: directional smoothing, conjugate smoothing, fluid vibrations, axi-symmetric problem, block scanning procedure, numerical integration, Abel transform

Introduction

In engineering, the integral Abel transform is often used in the analysis of spherically symmetric or axially symmetric objects. Abel transform is used in different optical applications – from calculation of radial mass distribution of galaxies [1] up to sizing of microscopic droplets in emulsions [2]. Abel transform plays a primary role in optical problems dealing with interpretation of fluid, gas or even two phase flow in circular transparent and semi-transparent tubes [3, 4].

Development of hybrid numerical – experimental techniques is an important method of analysis used for interpretation and validation of experimental results [5, 6], especially when such experimental techniques as laser holography is applied for investigation of high frequency vibrations of fluid [7, 8]. If the fluid dynamics is investigated in a tube the problem becomes even more complicated due to the complex geometry of the system. Abel transform must be exploited for the reconstruction of interference fringes due to the fact that the laser beam travels different lengths through the fluid at different positions of the laser rays penetrating through the surface of the tube [9, 10].

Such problems of fluid dynamics in vibrating tubes are found in many engineering applications. Typical examples are pipeline vibrations induced by fluid fow [11], fluid flow control by tube vibrations [12, 13], or even application of ultrasonic fluid vibrations for cleaning of blocked blood vessels [14].

The paper is comprised of several successive sections. First, numerical model for ideal compressible fluid without rotation is developed in axi-symmetric geometry. Next, fluid volumetric strains are obtained from the finite element model. Then, Abel transform is implemented and axi-symmetric geometry is evaluated. After that, the relationship between the intensity of laser beam in hologram plane and volumetric strains in vibrating fluid is developed. Finally, the results are discussed and conclusions are made.

Model of the system

The numerical model of fluid is developed on the basis of conventional finite element model based on the displacement formulation [15, 16]. Alternatively, the model of fluid could be developed using the velocity potential. But the displacement formulation has definite advantages over the velocity potential formulation as displacements are primary variables used in hybrid numerical – experimental techniques. Displacements become secondary variables in the velocity potential

formulation and should be determined in the secondary stage of analysis what would decrease the accuracy of the results. The main stages of the hybrid numerical – experimental procedure are presented in Fig. 1.

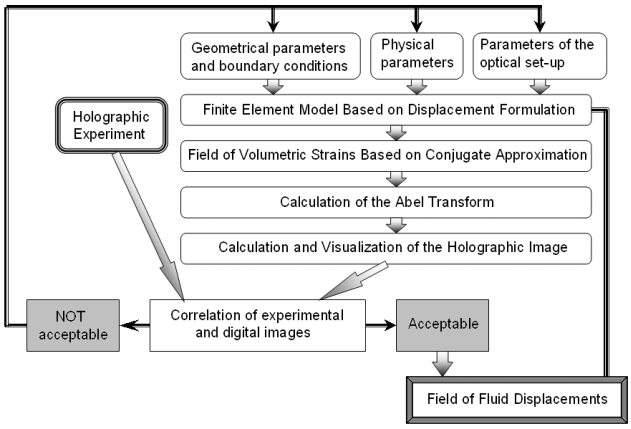

Fig. 1. Main stages of hybrid numerical – experimental procedure

First of all the finite element model for ideal compressible fluid without rotation is developed in axi-symmetric geometry. The mass matrix of the fluid is:

$$[M]=\int [N]^T \rho [N] 2\pi x dxdy\,, \tag{1}$$

where ρ is the density of the fluid in the status of equilibrium, x is radial co-ordinate; y is vertical co-ordinate (the axis of symmetry); $[N]$ is matrix of the shape functions determined by the following relationship:

$$\begin{Bmatrix} u \\ v \end{Bmatrix} = [N]\{\delta\}, \tag{2}$$

where u, v denote displacements of the fluid in the directions of x- and y-axes in the domain of appropriate finite element; $\{\delta\}$ is vector of nodal displacements. Explicitly:

$$[N]=\begin{bmatrix} N_1 & 0 & N_2 & 0 & \cdots \\ 0 & N_1 & 0 & N_2 & \cdots \end{bmatrix}, \tag{3}$$

where N_i are the shape functions of the analyzed finite element. The stiffness matrix of the fluid takes the following form:

$$[K]=\int \left([\overline{B}]^T \rho c^2 [\overline{B}] + [\tilde{B}]^T \lambda [\tilde{B}] \right) 2\pi x dxdy\,, \tag{4}$$

where c is the speed of sound in the fluid; λ is the penalty parameter for the condition of non-rotation. Matrix $[\overline{B}]$ relates volumetric strain with displacements and is defined from:

$$\frac{\partial u}{\partial x}+\frac{\partial v}{\partial y}+\frac{u}{x}=[\overline{B}]\{\delta\}. \tag{5}$$

Explicitly:

$$[\overline{B}]=\left[\frac{\partial N_1}{\partial x}+\frac{N_1}{x} \quad \frac{\partial N_1}{\partial y} \quad \frac{\partial N_2}{\partial x}+\frac{N_2}{x} \quad \frac{\partial N_2}{\partial y} \quad \cdots \right]. \tag{6}$$

Matrix $[\tilde{B}]$ is used to characterize rotation and is defined by the following equality:

$$\frac{\partial u}{\partial y}-\frac{\partial v}{\partial x}=[\tilde{B}]\{\delta\}. \tag{7}$$

Thus:

$$[\tilde{B}]=\left[\frac{\partial N_1}{\partial y} \quad -\frac{\partial N_1}{\partial x} \quad \frac{\partial N_2}{\partial y} \quad -\frac{\partial N_2}{\partial x} \quad \cdots \right]. \tag{8}$$

Conventional finite element analysis techniques are based on the approximation of nodal displacements via the shape functions. But volumetric strains (not nodal displacements) are involved in the relationships governing the intensity of illumination in the hologram. Thus the field of volumetric strain must be determined using the procedure of conjugate approximation with smoothing [17]. This procedure is adapted for calculation of volumetric strains for axi-symmetric problem of fluid vibrations.

First of all, theoretical field of volumetric strains $S_0(x,y)$ in the domain of appropriate finite element is calculated in the usual way:

$$S_0(x,y)=[\overline{B}]\{\delta_0\}, \tag{9}$$

where $\{\delta_0\}$ is the vector of nodal displacements corresponding to vibration of the fluid according to its eigenmode. Linear system of algebraic equations for the determination of smoothed nodal volumetric strains is constructed in analogy with the numerical technique developed in [17], but smoothing coefficient λ is replaced by matrix of orthotropic directional smoothing coefficients $[\hat{D}]$:

$$\begin{aligned} &\iint \left([\hat{N}]^T [\hat{N}] + [\hat{B}]^T [\hat{D}][\hat{B}] \right) 2\pi x dxdy \cdot \{\delta_v\} = \\ &= \iint [\hat{N}]^T S_0(x,y) 2\pi x dxdy, \end{aligned} \tag{10}$$

where double integral stands for the procedure of direct stiffness [18]; $\{\delta_v\}$ is the vector of smoothed nodal values of the volumetric strains $S_0(x,y)$; $[\hat{N}]$ is the row of the shape functions of a successive finite element:

$$\left[\hat{N}\right]=\left[N_1 \quad N_2 \quad ...\right], \tag{11}$$

$\left[\hat{B}\right]$ is the matrix of the first derivatives of the shape functions:

$$\left[\hat{B}\right]=\begin{bmatrix} \frac{\partial N_1}{\partial x} & \frac{\partial N_2}{\partial x} & \cdots \\ \frac{\partial N_1}{\partial y} & \frac{\partial N_2}{\partial y} & \cdots \end{bmatrix}, \tag{12}$$

$\left[\hat{D}\right]$ is the matrix of orthotropic directional smoothing coefficients:

$$\left[\hat{D}\right]=\begin{bmatrix} \lambda_x & 0 \\ 0 & \lambda_y \end{bmatrix}, \tag{13}$$

where λ_x is the radial smoothing coefficient and λ_y is the axial smoothing coefficient.

Calculation of the Abel transform comprises integration in the radial direction [9, 10]. It is determined that the radial smoothing coefficient can be much smaller than the axial smoothing coefficient due to this integration. Nevertheless, axial smoothing is essential in order to obtain holographic interferograms of acceptable quality for realistic finite element meshings. Thus the procedure of orthotropic directional smoothing enables to perform smoothing in the axial direction without unnecessary over-smoothing (with unavoidable distortions) in the radial direction.

The obtained volumetric strains are used in the procedure of numerical calculation of the Abel transform.

Numerical implementation of the Abel transform

Abel transform performs the projection of an axi-symmetric function to a plane [7, 9]:

$$\Phi(x,y)=\int_{-\infty}^{\infty}\varepsilon_v(r,y)dz\,. \tag{14}$$

Change of variables:

$$dz=d\sqrt{r^2-x^2}=\frac{rdr}{\sqrt{r^2-x^2}}, \tag{15}$$

yields:

$$\Phi(x,y)=2\int_{x}^{\infty}\varepsilon_v(r,y)\frac{rdr}{\sqrt{r^2-x^2}}\,. \tag{16}$$

The notation used is explained in detail in Fig. 2, where r is the radial coordinate. The upper integration limit is denoted as infinity in [7], but it is understood that the integration is performed only over the fluid domain.

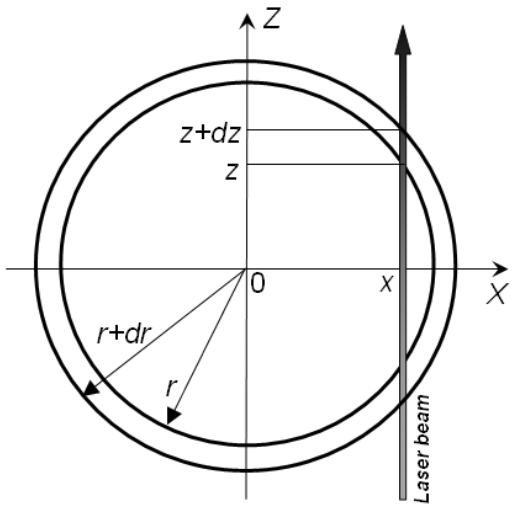

Fig. 2. Schematic diagram of the Abel transform

Numerical implementation of the calculation of the Abel transform is performed in three steps.

Step 1. The column number and the row number of a pixel with the corresponding value of the volumetric strain is obtained for all the analyzed values of the local coordinates for each finite element.

The calculations are performed for a sequential number of values of the local coordinates (ξ, η) of the finite element:

$$\xi=-1+\frac{2}{n-1}(i-1),\ i=1,\ldots,n,$$
$$\eta=-1+\frac{2}{n-1}(j-1),\ j=1,\ldots,n. \tag{17}$$

The plane orthogonal Cartesian coordinates x and y of these points are calculated using the shape functions of the analyzed finite element.

The digital image consists of the matrix of pixels where the columns are indexed from 0 to m_x and the rows are indexed from 0 to m_y. Thus a point (x, y) is mapped to the pixel (i_x, i_y):

$$i_x=round\left(\frac{x-x_{\min}}{x_{\max}-x_{\min}}m_x\right),$$
$$i_y=round\left(m_y-\frac{y-y_{\min}}{y_{\max}-y_{\min}}m_y\right). \tag{18}$$

Here the subscripts min and max denote the minimum and maximum values of the coordinates x and y. The procedure performing the shift to the coordinates of the center of the pixel (i_x, i_y) is performed:

$$x^*=i_x\frac{x_{\max}-x_{\min}}{m_x}+x_{\min},$$

$$y^* = y_{\min} - \left(i_y - m_y\right)\frac{y_{\max} - y_{\min}}{m_y}. \quad (19)$$

As the analyzed point of the structure does not necessarily coincide with the center of the pixel, further calculations are performed for the location of a point of the structure corresponding to the center of the pixel. The derivatives of the shape functions with respect to the local coordinates are multiplied by the nodal coordinates of the finite element:

$$\begin{bmatrix} \frac{\partial N_1}{\partial \xi} & \frac{\partial N_2}{\partial \xi} & \dots \\ \frac{\partial N_1}{\partial \eta} & \frac{\partial N_2}{\partial \eta} & \dots \end{bmatrix} \begin{bmatrix} x_1 & y_1 \\ x_2 & y_2 \\ \vdots & \vdots \end{bmatrix} = \begin{bmatrix} \frac{\partial x}{\partial \xi} & \frac{\partial y}{\partial \xi} \\ \frac{\partial x}{\partial \eta} & \frac{\partial y}{\partial \eta} \end{bmatrix}, \quad (20)$$

where x_i, y_i are the coordinates of the i - th node. The L – coordinates of the center of the pixel are obtained from:

$$\begin{bmatrix} x & x + \frac{\partial x}{\partial \xi} & x + \frac{\partial x}{\partial \eta} \\ y & y + \frac{\partial y}{\partial \xi} & y + \frac{\partial y}{\partial \eta} \\ 1 & 1 & 1 \end{bmatrix} \begin{Bmatrix} L_1 \\ L_2 \\ L_3 \end{Bmatrix} = \begin{Bmatrix} x^* \\ y^* \\ 1 \end{Bmatrix}. \quad (21)$$

Then the calculations are performed for the corrected local coordinates ($\xi+L_2$, $\eta+L_3$).

Step 2. For each scan line of the digital image the averaged volumetric strain for each pixel of the scan line is obtained. Schematic representation of this step of analysis is given in Fig. 3.

The implementation of this procedure is illustrated in Fig. 4.

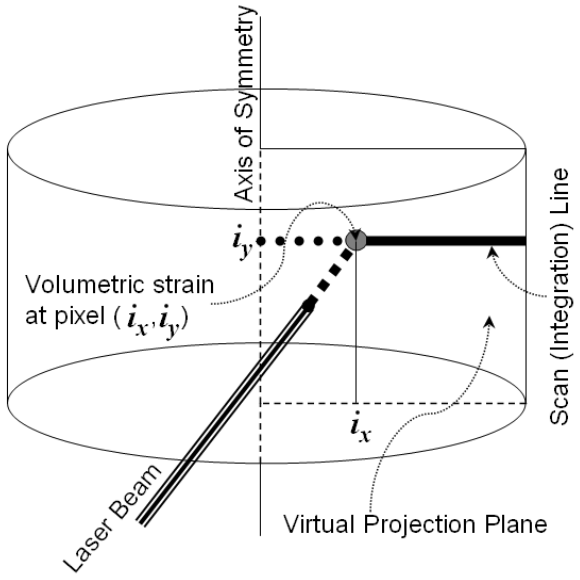

Fig. 3. Determination of volumetric strains for a scan line

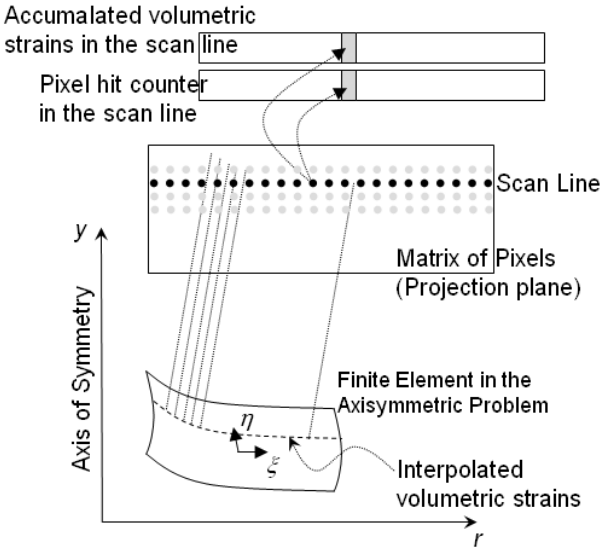

Fig. 4. Numerical implementation of the scanning procedure

The scanning of the file obtained in step 1 for each scan line of the digital image would be numerically rather not effective. In order to increase the numerical effectiveness of the procedure the block scanning procedure is implemented: the volumetric strains for a block of sequential scan lines are obtained while scanning the file from step 1. In our applications the block of 16 sequential scan lines was used. Thus the number of scans through the file obtained in step 1 is reduced.

Step 3. For each scan line of the digital image by using the right rectangle numerical integration rule the Abel transform is calculated and then the digital holographic image is produced.

Thus the Abel transform for the analyzed scan line is calculated in the following way:

$$\Phi_j = \sum_{i=j+1}^{n} 2\varepsilon_{vi} \frac{\left(x_{\min} + i\Delta\right)\Delta}{\sqrt{\left(x_{\min} + i\Delta\right)^2 - \left(x_{\min} + j\Delta\right)^2}}, \quad (22)$$

where Φ_j is the phase of the laser beam at the pixel j of the scan line, ε_{vi} is the volumetric strain at the pixel i of the scan line, $x_{\min}$ is the minimum value of the radial coordinate in the digital image, Δ is the radial distance between the adjacent pixels.

Numerical results

Axi-symmetric problem in a rectangular domain is analyzed. The right boundary is rigid and the displacements normal to it are set to zero. The left boundary is the axis of symmetry and the displacements normal to it are set to zero also. Periodic boundary conditions on the upper and lower boundaries are assumed: the displacements on those surfaces for the same values of the radial coordinate are assumed mutually equal.

As it is assumed that the cyclic frequency of excitation coincides with the eigenfrequency of the appropriate eigenmode and the excitation is not orthogonal to the

eigenmode, the excitation is not specified explicitly and vibrations according to the eigenmode are analyzed.

The unsmoothed digital stroboscopic holographic image of the seventh eigenmode is presented in Fig. 5. The smoothed digital stroboscopic holographic image of the seventh eigenmode is presented in Fig. 6. The necessity of smoothing is evident from those figures.

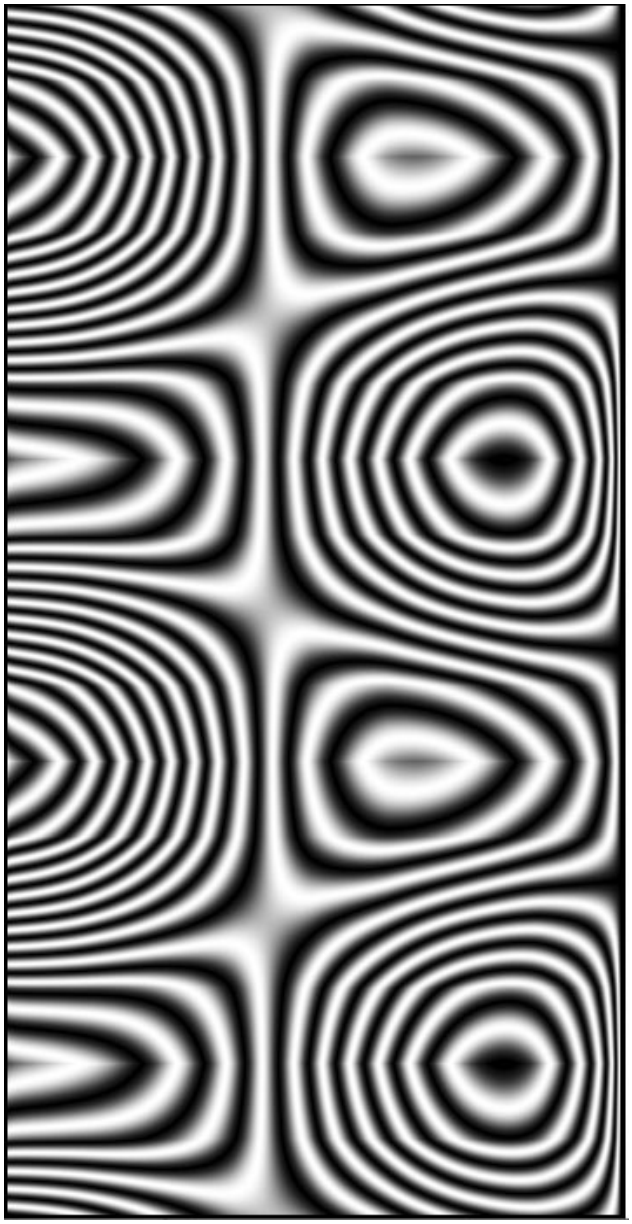

Fig. 5. Unsmoothed digital stroboscopic holographic image of the seventh eigenmode

Conclusions

The obtained digital holographic images of the vibrating fluid are used in the hybrid experimental – numerical procedure for the determination of the correlation with the experimental holographic images.

Numerical model for ideal compressible fluid without rotation is developed in axi-symmetric geometry. For the calculation of fluid volumetric strains from the finite element model the procedure of directional conjugate smoothing is proposed. The Abel transform is implemented in three steps:

1) the column number and the row number of a pixel with the corresponding value of the volumetric strain is obtained for all the analyzed values of the local coordinates for each finite element;

2) for each scan line of the digital image the averaged volumetric strain for each pixel of the scan line is obtained using the proposed block scanning procedure: the volumetric strains for a block of sequential scan lines are obtained while scanning the file from the previous step;

3) for each scan line of the digital image by using the right rectangle numerical integration rule the Abel transform is calculated and the digital holographic image is produced.

The necessity of smoothing is evident from the presented numerical results.

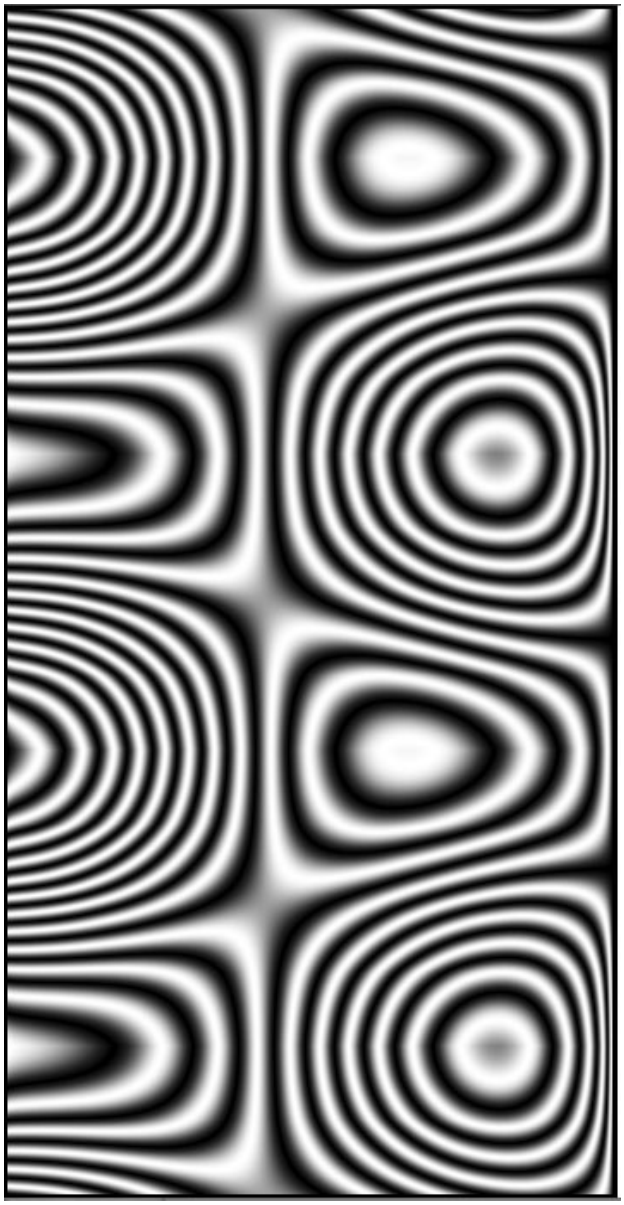

Fig. 6. Smoothed digital stroboscopic holographic image of the seventh eigenmode

References

[1] Binney J. and Tremaine S. (1987), *Galactic Dynamics*, Princeton University Press, Princeton.

[2] Hollingsworth K. G. and Johns M. L. (2005), "Spatially resolved emulsion droplet sizing using inverse Abel transforms", *Journal of Magnetic Resonance*, Vol. 176 No.1, pp. 71-8.

[3] Yousefian F. and Lallemand M. (1998), "Inverse radiative analysis of high-resolution infrared emission data for temperature and soecies profiles recoveries in axisymmetric semi-transparent media", *Journal of Quantitative Spectroscopy and Radiative Transfer*, Vol. 60 No. 6, pp. 921-31.

[4] Vanderwege B. A., O'Brien C. J. and Hochgreb S. (1999), "Quantitative shearography in axisymmetric gas temperature measurements", *Optics and Lasers in Engineering*, Vol. 31 No. 1, pp. 21-39.

[5] Rittel D. (2005), "A hybrid experimental–numerical investigation of dynamic shear fracture", *Engineering Fracture Mechanics*, Vol. 72 No. 1, pp. 73-89.

[6] Holstein A., Salbut L., Kujawinska M. and Juptner W. (2001), "Hybrid experimental – numerical concept of residual stress analysis in laser weldments", *Experimental Mechanics*, Vol. 41 No. 4, pp. 343-50.

[7] Vest C. M. (1979), *Holographic Interferometry, Chapter 3*, Wiley, New York.

[8] Lauterborn W. and Vogel A. (1984), "Modern optical techniques in fluid mechanics", *Annual Review Fluid Mechanics* Vol. 16, pp. 223-44.

[9] Houwing A., Takayama K., Koremoto K., Hashimoto T. and Mitobe H. (1983), "Finite fringe analysis of two dimensional and axially-symmetric flows", *Proc. of SPIE*, Vol. 398, pp. 174-80.

[10] Han J. H., Kennaugh A. and Poll D. I. A. (1997), "Visualization of non-equilibrium dissociating flows", *Journal of Aerospace Engineering*, Vol. 211 No. G5, pp. 295-305.

[11] Zou G. P., Cheraghi N. and Taheri F. (2005), "Fluid-induced vibration of composite natural gas pipelines", *International Journal of Solids and Structures*, Vol. 42 No. 3-4, pp. 1253-68.

[12] Oz H. R. and Boyaci H. (2000), "Transverse vibrations of tensioned pipes conveying fluid with time-dependent velocity", *Journal of Sound and Vibration*, Vol. 236 No. 2, pp. 259-76.

[13] Ragulskis M., Fedaravičius A. and Ragulskis K. (2006), "Harmonic balance method for FEM analysis of fluid flow in a vibrating pipe", *Communications in Numerical Methods in Engineering*, Vol. 22 No. 4, pp. 347-56.

[14] Rabiner R. and Hare B. A. (2003), "Ultrasonic device for tissue ablation and sheath for use therewith", *Acoustical Society of America Journal*, Vol. 114 No. 2, p. 572.

[15] Iershov N. F. and Shahvierdi G. G. (1984), *The Method of Finite Elements in the Problems of Hydrodynamics and Hydroelasticity*, Sudostroienie, Leningrad.

[16] Zienkiewicz O. C. and Taylor R. L. (2000), *The Finite Element Method. Volume 3. Fluid Dynamics*, Wiley, UK.

[17] Ragulskis M. and Ragulskis L. (2004), "Conjugate approximation with smoothing for hybrid photoelastic and FEM analysis", *Communications in Numerical Methods in Engineering*, Vol. 20 No. 8, pp. 647-53.

[18] Bathe K. J. (1982), *Finite Element Procedures in Engineering Analysis*, Prentice-Hall, Englewood Cliffs.